Performance Evaluation in Bluetooth Dense Piconet Areas

Franco Mazzenga, Dajana Cassioli, *Member, IEEE*, Andrea Detti, Ibrahim Habib, Pierpaolo Loreti, and Francesco Vatalaro, *Senior Member, IEEE*

***Abstract*—Bluetooth is a low-cost, short-range wireless technology capable of providing many communication functionalities, ranging from wire replacement to simple personal area networking. In Bluetooth local networking applications, a critical issue still under study is the evaluation of the network performance when multiple piconets are simultaneously active in the same area, thus, causing mutual interference. In this paper, we provide a closed-form expression for the packet loss probability in Bluetooth dense piconet area accounting for capture effects due to propagation losses. The effectiveness of the proposed approach is assessed by comparing the analytical results with those obtained from Monte Carlo simulations. By considering different scenarios, we show the dependence of results on the geometry and on the characteristics of the environment. It is observed that packet loss probability can significantly change with the position of the reference receiver in the area, as well as with the extension of the piconets area as compared with the coverage area of the receiver. We use the packet loss probability to evaluate the upper and the lower bounds of the network aggregate throughput and the average packet transmission time. Due to propagation effects, large variations of these parameters with the position of the reference receiver in the area are evidenced.**

***Index Terms*—Cochannel interference, communication system performance, personal communication networks.**

NOMENCLATURE

$R(R)$	Reference receiver.
$P(M)$	Outage probability due to M interfering piconets.
W_T	Bluetooth terminal transmitted power.
W_R	Power received by the reference receiver.
U_m	Interference power in the RR due to the mth piconet.
I_M	Aggregate interference power in the RR due to M interfering piconets.
N	Thermal noise power.
ρ_0	Target signal to noise ratio.
p	Probability that an interfering Bluetooth device is transmitting on the frequency where the RR is tuned.
t_S	Bluetooth time slot duration.
$T(M)$	Average aggregate throughput due to M piconets in the area.
τ_{MS}	Average transmission time from Master to Slave.
τ_{SM}	Average transmission time from Slave to Master.

Manuscript received May 4, 2003; revised July 8, 2003 and September 29, 2003; accepted October 1, 2003. The editor coordinating the review of this paper and approving it for publication is E. Hossain. Work done within *RADIOLABS*, Consorzio Università Industria-Laboratori di Radiocomunicazioni, Italy. This paper was presented in part at the ICC 2002.

F. Mazzenga, A. Detti, and F. Vatalaro are with the Dipartimento di Ingegneria Elettronica-University of Rome "Tor Vergata," 00133 Rome, Italy (e-mail: mazzenga@ing.uniroma2.it; pierpaolo.loreti@uniroma2.it; vatalaro@uniroma2.it).

D. Cassioli is with the Consorzio Università Industria Laboratori di Radiocomunicazioni (Radiolabs), Electronic Engineering Department-University of Rome "Tor Vergata," 00133 Rome, Italy (e-mail: cassioli@ing.uniroma2.it).

P. Loreti is with the Consorzio Nazionale Interuniversitario per le Telecomunicazioni (CNIT)-University of Rome "Tor Vergata," 00133 Rome Italy (e-mail: andrea.detti@uniroma2.it).

I. Habib is with the Department of Electrical Engineering City University of New York, New York, NY 10031 USA (e-mail: habib@ccny.cuny.edu).

Digital Object Identifier 10.1109/TWC.2004.837395

I. INTRODUCTION

THE INCREASING importance of internet web-based data applications and the pressing request for mobility pushed the research activities toward the definition of new global radio access networks.

Wireless personal area networks (PANs) represent the first access level to the global network. Equipment suitable for PAN communications is low-cost, provides communications among very different appliances, and interfaces with wired and wireless external networks. In a typical domestic or office environment, several communicating appliances and/or terminals accessing to the internet coexist and their position cannot be easily predicted. Therefore, proper selection of a suitable wireless technique to connect them is mandatory. Furthermore, to ensure full connectivity, this radio technology should be able to dynamically create and to manage ad-hoc networks among the communicating terminals in the area. Ad-hoc wireless networks allow terminals to flexibly and autonomously organize themselves to communicate without a pre-existing infrastructure.

Bluetooth is a transmission standard designed to support ad-hoc connectivity in a local area [1]. When Bluetooth terminals get close enough, they can cluster into one *piconet*, and temporarily designate a master unit to coordinate transmissions with up to seven slave units. Bluetooth is based on packet transmission and frequency hopping (FH) technologies to provide channelization among different piconets within the same area. Terminals belonging to the same piconet communicate over the channel identified by a frequency hopping code. According to the Bluetooth standard, terminals are allowed to hop within up to 79 bands in the unlicensed 2.4 GHz Industrial-Scientific-Medical (ISM) band [2]. Based on different FH code patterns, several piconets can coexist in the same area. Typical scenarios are conference halls or airports that gather a large number of people willing to connect their portable terminals to other terminals, or to the fixed network access points. In these cases, the terminals aggregate randomly to form a large number of piconets with a different number of slaves per piconet. In

such a dense piconet area, packet collisions can occur with significant probability thus, degrading link performance and reducing the overall throughput.

The parameter accounting for these effects is packet loss probability (PLP). Some contributions have been already provided in the literature to evaluate interference effects on Bluetooth performance and/or to evaluate the PLP [3], [6]. Lim *et al.*[3] considered a simple Bluetooth network and evaluates the throughput and delay using a simple upper bound on PLP. In [4] and [5], the Bluetooth network throughput is analyzed through simulations. In [5] some modifications to some Bluetooth protocol parameters were proposed to improve the throughput. In [3] and [5], the environment characteristics and the spatial distribution of terminals that render the network performance parameters inhomogeneous over the area have not been considered in PLP evaluation. A first attempt to account for spatial distribution of the users in the PLP, calculation was made in [7] where a closed form for the PLP was obtained under Poisson traffic assumption and assuming simple propagation models. Another analytical approach for the calculation of PLP was presented in [6], but results were obtained by restricting the number of overlapping piconets to three and still assuming a simple propagation model. Finally, a worst case analysis was provided in [8] which led to an upper bound for the PLP, similar to that presented in [3], without considering the mitigation effects of propagation losses.

In this paper, we provide a semi-analytical approach to evaluate PLP accounting for the geometry of the environment, its propagation characteristics, and for the position of the Reference Receiver (RR) in the area. The PLP formulation obtained in this paper is different from that in [7] and, as shown in the following, many of the (restrictive) assumptions indicated in [7] can be easily removed using the proposed semi-analytical approach. We expand the derivation of the results presented in [9], and we use PLP to evaluate the upper and the lower bounds for the network aggregate throughput and the average packet transmission time.

The paper is organized as follows. In Section II we first derive a closed-form expression for the PLP, and then we illustrate the numerical procedures to evaluate it. In Section III, we define the network performance parameters. In Section IV, we provide some simulation results to validate the proposed approach and we evaluate PLP for different scenarios. We use PLP to plot the upper and the lower bounds of the considered network performance parameters. Finally, in Section V, we draw our conclusions.

II. Evaluation of Packet Loss Probability

We consider a dense piconet area with $M+1$ piconets. PLP is defined as the probability that the signal to interference plus noise ratio at the output of the RR falls below a threshold, ρ_0, which accounts for the fast fading characteristics of the environment, i.e.,

$$P(M) = Prob\left\{\frac{W_R}{I_M + N} \le \rho_0,\right\} = \int_{-\infty}^{0} f_{Z_M}(x)dx \quad (1)$$

where W_R is the received power at the RR, and I_M and N are the interference due to the M interfering piconets in the area and the thermal noise power, respectively. In (1), $f_{Z_M}(x)$ is the probability density function (pdf) of $Z_M = W_R - \rho_0(I_M + N)$ and we have [10]

$$f_{Z_M}(x) = f_{W_R}(x) \otimes \frac{1}{\rho_0} f_{I_M}\left(-\frac{x}{\rho_0}\right) \otimes f_N\left(-\frac{x}{\rho_0}\right) \quad (2)$$

where $\otimes$ denotes convolution and $f_{W_R}(x)$, $f_{I_M}(x)$ and $f_N(x)$ are the pdf's of W_R, I_M and N, respectively. In this section, we present a novel semi-analytical procedure to evaluate (1).

A. Interference Characterization

Packet collisions take place when two or more piconets simultaneously transmit in the same frequency time slot. Depending on the dimensions of the area where piconets are located, propagation distance can mitigate interference effects due to collisions. The FH patterns assigned to the different piconets can be modeled as statistically independent time-discrete random sequences assuming values in the set $\{f_0, f_1, \ldots, f_{N_f-1}\}$. The N_f frequencies f_i are the carrier frequencies used for hopping. We assume that each Bluetooth unit transmits with the same power level W_T (i.e., absence of power control) and that each interfering unit can be arbitrarily located in the area. The overall interference power, I_M, suffered by the RR due to the M active piconets is

$$I_M = \sum_{m=1}^{M} \chi_m U_m \quad (3)$$

where χ_m, $m = 1, \ldots, M$, are independent, identically distributed, binary random variables (rv) accounting for the occurrence of the frequency-collision events, and U_m is the power received at the RR due to a transmitter belonging to the m-th piconet. We can model χ_m as

$$\chi_m = \begin{cases} 1, & \text{with probability } p_m \\ 0, & \text{with probability } q_m \end{cases} \quad (4)$$

where p_m is the probability that the mth piconet in the area transmits on the same frequency slot of the RR and $q_m = 1 - p_m$. We only consider the case of one-slot packet transmission [2], and we assume that each slot always contains a packet whose duration can be lower or equal to the time slot, t_S. In this case we have [8]

$$p_m = \begin{cases} \frac{1}{N_f} & \text{synchronized piconets} \\ 1 - \left(1 - \frac{1}{N_f}\right)^2 & \text{nonsynchronized piconets} \\ 1 - \left(2(1-\lambda)\left(1 - \frac{1}{N_f}\right) + (2\lambda - 1)\left(1 - \frac{1}{N_f}\right)^2\right) & \text{packet length less than time slot} \end{cases} \quad (5)$$

where λ is the ratio between the packet duration and the time slot duration t_S.[1] The probabilities p_m in (5) were obtained starting

[1]Piconets are considered synchronized when time slots of the piconets start at the same time instant; otherwise they are nonsynchronized.

from the calculation of the packet collision probabilities conditioned to the time difference between the clocks of the reference master and the interfering master. Then results were averaged with respect to the clocks time difference assumed to be a rv uniformly distributed in $[0, t_S)$. From (5), we observe that p_m are independent of m (in the following, we indicate p_m with p) and, consequently, the pdf of χ_m in (4) is independent of m. The p_m in (5) can be easily modified to account for packet source activity as indicated in [8].[2]

To account for the interference due to piconets transmitting on two adjacent frequencies f_{n-1} and f_{n+1} where f_n is the frequency of the RR, the χ can be modeled as

$$\chi = \begin{cases} 1 & \text{with probability } p \quad \text{(co-channel interference)} \\ \alpha & \text{with probability } p_\alpha \\ & \quad \text{(adjacent channel interference)} \\ 0 & \text{with probability } q = 1 - p - p_\alpha \end{cases}$$

where the attenuation factor α accounts for the selectivity of the transmission filters [4]. From the independence assumption of the frequency hopping patterns it can be shown that $p = 1/N_f$, $p_\alpha \cong 2(N_f - 1)/N_f$. In the following no adjacent channel interference is considered, but the derivation of the PLP can be easily extended to this case.

The interference powers, U_m $m = 1, \ldots, M$ depend on the propagation losses due to the transmitter-receiver distance and on the geometry of the obstacles. Therefore

$$U_m = W_T \cdot L_m \cdot S_m, \qquad m = 1, \ldots, M, \tag{6}$$

where we evidenced a deterministic component L_m, usually referred to as *path loss*, which depends on the transmitter-receiver distance, and a random component, S_m, accounting for shadowing.

In general, the overall propagation loss depends on the position of the RR and on the position of the mth interferer. Since the signal transmitted by each interfering user goes through the same propagation environment, the statistics of the interfering power measured at the RR can be assumed to be independent of m, i.e., the pdf's of $L_m \cdot S_m$ and thus, U_m, do not depend on m.

When the map of the coverage area is available, L_m could be evaluated using ray-tracing techniques for each position of the RR and of the interferer (see Fig. 1). However, in the following we restrict our analysis to a two-dimensional (2-D) environment and we assume that L_m only depends on the distance d_m of the interferer from the RR.

B. Calculation of Packet Loss Probability

Assuming that $f_U(x)$ and $f_{W_R}(x)$ are known, the PLP due to M interfering piconets in the area is given in (1) and using (3), Z_M is

$$Z_M = W_R - \rho_0 N - \rho_0 \sum_{m=1}^{M} \chi_m U_m. \tag{7}$$

[2]Indicating with G and $G \leq 1$ the packet source activity, in the synchronized piconets case, the collision probability p is $p = G/N_f$. The results for the other cases can be found in [8].

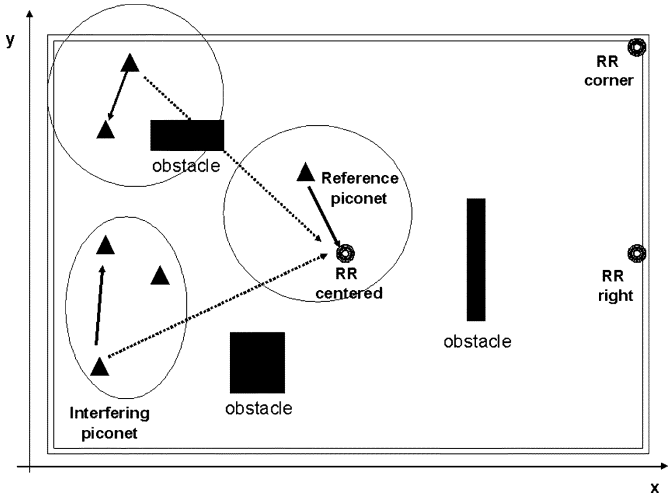

Fig. 1. Example of a geometrical arrangement in the local area.

From (7), the following recursive equation in the number of piconets holds

$$Z_M = Z_{M-1} - \varepsilon_M \tag{8}$$

where $\varepsilon_M = \rho_0 \chi_M U_M$ is the additional interference contribution due to the M-th piconet and $Z_0 = W_R - \rho_0 N$. Without loss of generality, in the following derivations, we omit the noise power N. Thus, the pdf of Z_M is

$$f_{Z_M}(x) = f_{W_R}(x) \otimes f_{\varepsilon_1}(-x) \otimes \cdots \otimes f_{\varepsilon_M}(-x) \tag{9}$$

with $f_{Z_0}(x) = f_{W_R}(x)$[3] and $f_\varepsilon(x) = f_{\varepsilon_i}(x)$ for $i = 1, 2, \ldots, M$, is:

$$f_\varepsilon(x) = q\delta(x) + \frac{p}{\rho_0} f_U\left(\frac{x}{\rho_0}\right) \tag{10}$$

where $\delta(x)$ is the Dirac delta function.

Using (9) and (10), after some calculations (see Appendix A), the following general expression for the packet loss probability is obtained

$$P(M) = \sum_{k=1}^{M} \binom{M}{k} q^{M-k} p^k \beta_k \tag{11}$$

where p is given in (5) and $q = 1 - p$. The coefficients β_k are

$$\beta_k = \int_{-\infty}^{0} g_k(x) \otimes f_{W_R}(x) dx \tag{12}$$

where $g_k(x) = \rho_0^{-k} f_{U_1}(-x/\rho_0) \otimes \cdots \otimes f_{U_k}(-x/\rho_0)$ for $k = 1, 2, \ldots, M$, and $g_0(x) = \delta(x)$. The term $\binom{M}{k} q^{M-k} p^k$ is the probability that k among the M interfering piconets are transmitting on the same RR frequency. The coefficients β_k in (11) accounts for the PLP reduction due to the environment propagation characteristics, e.g., path loss and shadowing. In fact, from

[3]Assuming that the noise power N is constant we obtain $f_{Z_0}(x) = f_{W_R}(x) \otimes \delta(x + \rho_0 N) = f_{W_R}(x + \rho_0 N)$ i.e., the pdf of Z_0 is a translated version of $f_{W_R}(x)$.

the definition, it can be observed that β_k is always less than unity for each k, and increases with k approaching to one as k tends to infinity. Furthermore, as shown in the following, the coefficients β_k depend on the position of the RR and on the dimensions of the network area as compared to the RR coverage area.

In the case of $\beta_k = 1$, for each k, the upper bound in [8] is reobtained as

$$P(M) = \sum_{k=1}^{M} \binom{M}{k} q^{M-k} p^k \beta_k \leq 1 - q^M. \tag{13}$$

Equation (13) can be conveniently rewritten as

$$P(M) = 1 - q^M - \sum_{k=1}^{M} \binom{M}{k} q^{M-k} p^k (1 - \beta_k). \tag{14}$$

Equation (14) can be used to obtain successive approximations for the PLP by neglecting the terms corresponding to β_k that are very close to unity. This can be useful for large M when it can be difficult to obtain a good numerical approximation for β_k.

The PLP calculation procedure (2)–(13) and the corresponding PLP results are still valid when only packets with duration of 3 (or 5) time slots are transmitted. This is due to the fact that even in these cases, the change of the transmission frequency always occurs at the end of the packet independently of its length.

C. Calculation of Packet Loss Probability Parameters

To calculate β_k, the probability density functions $f_{W_R}(x)$ and $f_U(x)$ are needed. In general, it is very difficult to evaluate them in closed form. For this reason, we consider numerical approximations for $f_U(x)$ and for $f_{W_R}(x)$ obtained starting from a spatial discretization of the network area as illustrated in Appendix B. For $f_U(x)$ we assume

$$f_U(x) = \sum_{k=1}^{K} \pi_k \delta(x - \Pi_k) \tag{15}$$

where Π_k are the discrete values of U, K is an integer, and the probabilities π_k, $k = 1, \ldots, K$ are evaluated as (see Appendix)

$$\pi_k = \frac{1}{A} \sum_{i=0}^{N_x - 1} \sum_{l=0}^{N_y - 1} \Xi(x_i, y_l | U \in \Omega_k, (x_i, y_l) \in S_A)\, \Delta x \Delta y \tag{16}$$

where N_x and N_y are the number of points along the x and y axes, respectively, located in the grid, superimposed on the local area (see Fig. 2); A is the surface of the network area; $\Xi(x, y | U \in \Omega_k, (x, y) \in S_A)$ is an indicator function identifying the points within the piconets area S_A such that the interference power U, received by the RR, lies in the interval Ω_k (see Appendix B).

To characterize the pdf of the received power $f_{W_R}(x)$, we follow the same approach thus, obtaining

$$f_{W_R}(x) = \sum_{j=1}^{J} \gamma_j \delta(x - \Gamma_k) \tag{17}$$

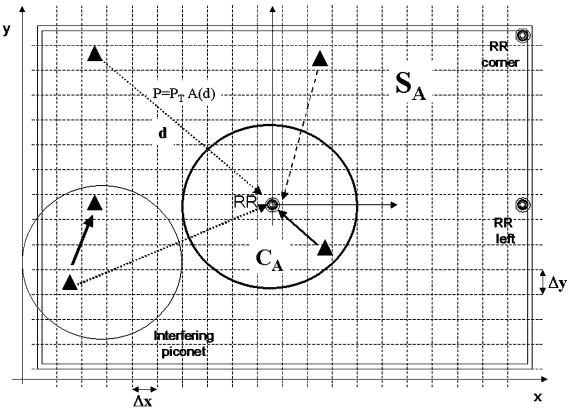

Fig. 2. Gridded area used to evaluate the probabilities of interference and power levels.

where Γ_k are the discrete values of W_R, J is an integer and the probabilities γ_j, $j = 1, \ldots, J$, are calculated as

$$\gamma_j = \frac{1}{A} \sum_{i=0}^{N_x - 1} \sum_{l=0}^{N_y - 1} \Xi(x_i, y_l | W_R \in \Omega_j, (x_i, y_l) \in S_A \bigcap C_A) \Delta x \Delta y. \tag{18}$$

It should be observed that the indicator function Ξ now accounts for both the piconets area S_A and the coverage area C_A of the RR. The C_A extension can be calculated from link budget starting from the path loss model and the shadowing statistics. The proposed numerical approach to evaluate $f_U(x)$ and $f_{W_R}(x)$ is quite general and can be used for any type of environment and for any configuration of obstacles in the area. The presence of obstacles in the area restrict the available positions of the interferers and of the RR in the area and this is accounted in the calculation of π_k and γ_j in (16) and (18) (see Appendix B).

III. Network Performance Parameters

In this section, we define the aggregate throughput and the average packet transmission time. In the following derivations, we assume that piconets in the area have the same number of slaves N_S, and that fixed length packet are used for transmission (such as the DM1 packet,[4]; see [2]). Slaves are always transmitting to the master in their time slots and the master always transmits to each slave in accordance to a round-robin scheduling. No signalling information is exchanged over the radio interface.

A. Aggregate Throughput

Starting from the previous assumptions and indicating with C, the overall radio capacity in the piconet measured in packet per second, in an error free environment the master gets $C/2$ and each slave gets $C/(2N_S)$. Nevertheless, in an error prone environment, these capacities are not fully exploited due to the PLP. We define the throughput of a single master-slave connection as the mean number of packets successfully received in the time unit. The total piconet throughput is the sum of the

[4]The DM1 packet supports a data payload from 0 to 17 bytes with CRC, 2/3 FEC, and is transmitted within one time slot.

throughput for all connections in the piconet. In the following we analyze the master-to-slave and the slave-to-master directions separately.

The total piconet throughput in the master to slave direction (e.g., T_{MS}) is

$$T_{MS}(M, x_1, y_1, \ldots, x_{N_S}, y_{N_S}, N_S) = \frac{C}{2N_S} \sum_{l=1}^{N_S} (1 - P(x_l, y_l, M)) \quad (19)$$

where (x_l, y_l), $l = 1, 2, \ldots, N_S$ are the slaves coordinates in the piconets area.

Due to the Bluetooth mechanisms [2], a slave is allowed to transmit to the master only when it receives a packet from the master. Thus, when a master packet is lost, the return slot is wasted. Accounting for this mechanism the throughput of the piconet in the slave to master direction is

$$T_{SM}(M, x_1, y_1, \ldots, x_{N_S}, y_{N_S}, X, Y, L) = \frac{C}{2N_S} \cdot \sum_{l=1}^{N_S} (1 - P(x_l, y_l, M))(1 - P(X, Y, M)) \quad (20)$$

where the capitals (X, Y) indicate the master coordinates. Hence, the total throughput of the piconet can be calculated as

$$T_P(M, x_1, y_1, \ldots, x_{N_S}, y_{N_S}, X, Y, N_S) = T_{MS} + T_{SM} \quad (21)$$

where, for notational simplicity, we omitted the indication of the dependencies on the right side of (21).

Fixing the master position (X, Y) in the area and assuming that slaves' coordinates are independently randomly generated, we define the piconet average throughput as

$$\overline{T}_P(M, X, Y) = \int \cdots \int T_P \, g(x_1, y_1 | X, Y) \cdot g(x_{N_S}, y_{N_S} | X, Y) \, dx_1 dy_1 \cdots dx_{N_S} dy_{N_S} \quad (22)$$

where the integral in (22) is extended to the master coverage area and $g(x_i, y_i | X, Y) = g(x_1, y_1 | X, Y)$, $i = 2, \ldots, \max(2, N_S)$ are the pdf of the slaves' coordinates given the master position, (X, Y).

We define the average aggregate throughput of all the piconets in the area by averaging (22) with respect to the master coordinates, i.e.,

$$T(M) = \int \int \overline{T}_P(M, X, Y) \, f(X, Y) dX dY \quad (23)$$

where the integral in (23) is extended to the piconets area and $f(X, Y)$ is the density of the masters. Considering M masters uniformly distributed in the area, we have $f(X, Y) = M/A$.

The calculation of (23) heavily depends on the propagation characteristics in the piconets area not allowing to outline general conclusions. Therefore, to give an idea of the throughput variability with the area dimensions, we resort to simple upper and lower bounds. Indicating with $P_{\min}(M)$ and $P_{\max}(M)$, the minimum and the maximum PLP in the piconets area, using them in (23) we obtain

$$MC(1 - P_{max}(M)) \left(1 - \frac{P_{max}(M)}{2}\right) \leq T(M) \leq MC(1 - P_{min}(M)) \left(1 - \frac{P_{min}(M)}{2}\right). \quad (24)$$

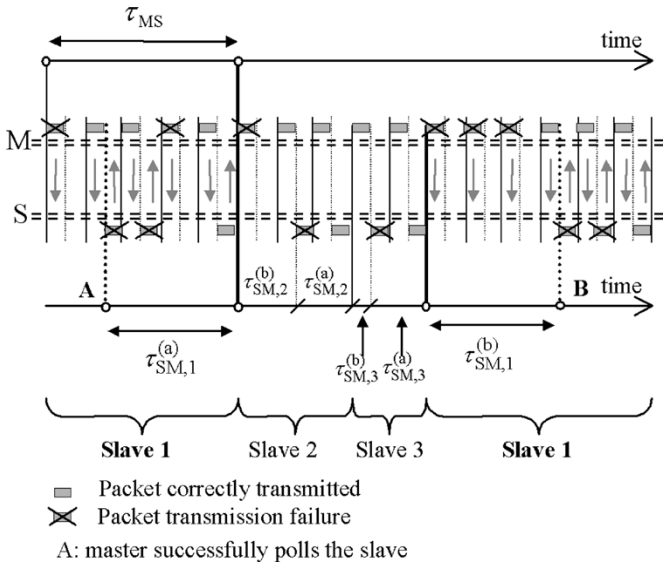

Fig. 3. Slave to master transmission. A-B: Example of transmission time in the slave-to-master direction considering three slaves in the piconet.

B. Average Packet Transmission Time

We define the packet transmission time as the time interval between the start of the packet transmission and the reception of the related acknowledgment (ACK) message (see Fig. 3). To evaluate the packet transmission time, we consider a single master-slave connection, and we analyze the master-to-slave (MS), and the slave-to-master (SM) directions separately.

Considering the master-to-slave direction we have

$$\text{Prob}\{\tau_{MS} = 2(n+1)t_S\} = (1 - P(X, Y, M))(1 - P(x, y, M)) \cdot [P(X, Y, M) + (1 - P(X, Y, M)) P(x, y, M)]^n, \quad n = 0, 1, 2, \ldots \quad (25)$$

where (X, Y) and (x, y) are the master and the slaves coordinates, respectively; M is the number of piconets in the area and t_S is the time slot duration. Equation (25) is obtained, assuming that the master continuously retransmits the packet to the slave until the ACK is received (no timeout are considered). As a consequence the average packet transmission time conditioned to the master and to the slave coordinates is

$$E\{\tau_{MS}\} = \sum_{n=0}^{\infty} 2(n+1)t_S \text{Prob}\{\tau_{MS} = 2(n+1)t_S\} = \frac{2t_S}{(1 - P(x, y, M))(1 - P(X, Y, M))}. \quad (26)$$

The $E\{\tau_{MS}\}$ depends on the master and the slave coordinates. Thus, to obtain the upper and the lower bounds for (26), we again consider $P_{\min}(M)$ and $P_{\max}(M)$ in the area thus obtaining:

$$\frac{2t_S}{(1-P_{min}(M))^2} \leq E\{\tau_{MS}\} \leq \frac{2t_S}{(1-P_{max}(M))^2}. \quad (27)$$

To evaluate the average transmission time in the slave to master direction, we consider the situation depicted in Fig. 3. The slave can start the packet transmission when it is polled by the master, and the corresponding ACK is contained in the subsequent master polling packet. Thus, the number of slaves and the polling scheme influence the calculation of this time interval.

When the master successfully polls the slave 1 (point A in Fig. 3), the time interval required from the slave to correctly transmit a new packet to the master is a random variable indicated with $\tau^{(a)}_{SM,1}$ and its probability distribution is (28) (see equation at bottom of page). The slave 1 receives the ACK packet only when it is polled again and the packet with the poll is successfully received (point B in Fig. 3). Indicating with $\tau^{(b)}_{SM,1}$ the time required by the master to successfully re-poll the slave 1, we obtain

$$\begin{aligned}&\text{Prob}\left\{\tau^{(b)}_{SM,1} = (2n+1)t_S\right\}\\ &\quad = (1-P(x,y,M))\,P(x,y,M)^n \quad n=0,1,2,\ldots \quad (29)\end{aligned}$$

Thus, considering the slave number 1, the total packet transmission time (segment A-B in Fig. 3) from slave to master is

$$\tau_{SM,1} = \tau^{(a)}_{SM,1} + \tau^{(b)}_{SM,1} + \sum_{i=2}^{N_S}\left(\tau^{(a)}_{SM,i} + \tau^{(b)}_{SM,i}\right). \quad (30)$$

Taking the average of (30), we obtain

$$\begin{aligned}E\{\tau_{SM,1}\} = \ldots &= E\left\{\tau_{SM,N_S}\right\}\\ &= \frac{2N_S t_S}{(1-P(x,y,M))(1-P(X,Y,M))}. \quad (31)\end{aligned}$$

Apart for the scaling factor N_S, the upper and the lower bounds for (31) can be easily obtained from (27).

IV. Simulation Results

A. Validation of the Proposed Approach

In this subsection, we describe the simulation procedure adopted to compare the theoretical and simulation results, in terms of PLP for a Bluetooth dense piconet area in a typical high interference scenarios. We performed Monte Carlo simulations to evaluate the effects of piconet self-interference only. In each snapshot, we generate M masters uniformly located in the area. Each master forms a piconet with N_S active slaves, where N_S is a random number, uniformly distributed between 1 and 7. Following the recommendations in [2], the transmitted power W_T is set to 1 mW. We assumed the following dual slope model for path loss, [11]

$$\begin{aligned}L_m(d) &= L(d)\\ &= \begin{cases}20\cdot\log\left(\frac{4\pi d}{\lambda}\right)\\ \quad \approx 40+20\log(d), & d\leq 8.5\text{ m}\\ 36\cdot\log\left(\frac{4\pi d}{\lambda}\right)\\ \quad \approx 25.3+36\log(d), & d>8.5\text{ m}\end{cases}\\ &\quad m=1,2,\ldots,M \quad (32)\end{aligned}$$

where $L(d)$ is in dB, d in m. Neglecting noise and shadowing and assuming a receiver sensitivity of -70 dBm, using (32) for link budget, we obtain a circular coverage area C_A with radius 17.6 m. The N_S slaves participating in each piconet are located randomly, according to a uniform distribution in the piconets area. The N_S slaves within a circular area of 35.2 meters diameter, centered in the position of the piconet master, are considered as connected to the selected master. The reference signal to noise target was assumed $\rho_0 = 11$ dB. Each piconet transmission begins in a randomly selected time slot. In every piconet, the master begins the transmission by sending an ACL packet to one of the N_s slaves belonging to its piconet. We considered the conventional round-robin scheduling policy. For each master, we randomly generated its own channel hopping sequence, assuming a uniform distribution over the 79 frequency-carriers. The length of the frequency hopping sequence for each master was taken equal to the duration of the simulation snapshot. We averaged the performance metrics over a large number of simulation snapshots for each scenario. In each snapshot, we regenerated the users' positions. In each time slot, we compute the signal-to-interference ratio of the RR. When the interference I is zero, i.e., terminals in the interfering piconets transmit over different frequencies, we assume that no packet loss occurs, since we assumed that the transmitter is in the coverage of the RR. In Figs. 4 and 5, the PLP obtained by Monte Carlo simulations are compared with the results of the proposed semi-analytical procedure [see (11)]. We considered different positions of the RR, as illustrated in Fig. 1. The semianalytical results shown in Figs. 4 and 5 were obtained assuming for both W_R and U a discrete pdf as in (15) and (17) (see Appendix B) based on the following values (in dBm): $\Gamma_k = \Pi_k = \Pi_1 + k\Delta$ where k is an integer and Δ (dBm) is the power step increment. We assumed $\Pi_1 = -80$ dBm and the maximum values for W_R and

$$\text{Prob}\left\{\tau^{(a)}_{SM,1} = (2n+1)t_S\right\} = \begin{cases}(1-P(x,y,M)) & n=0\\ P(x,y,M)\,(1-P(x,y,M))\,(1-P(X,Y,M))\\ \quad\cdot\left[P(X,Y,M)+(1-P(X,Y,M))\,P(x,y,M)\right]^{n-1} & n>0\end{cases} \quad (28)$$

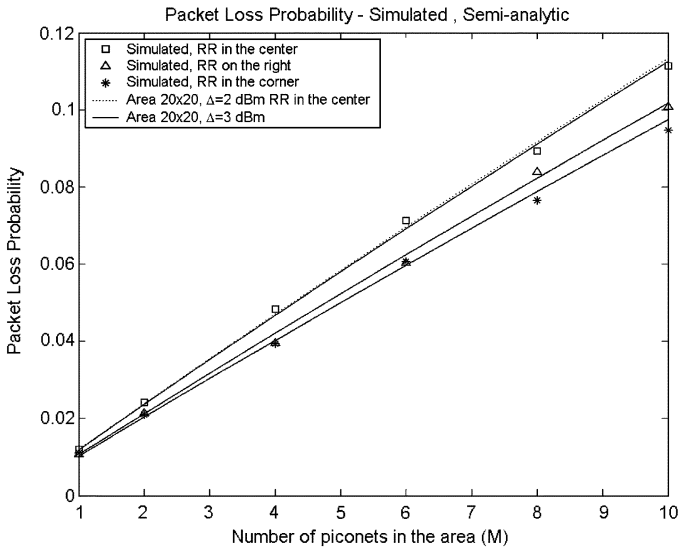

Fig. 4. Packet loss probability versus the number of piconets in the area. Square area: $20 \times 20\ \mathrm{m}^2$, synchronized piconets.

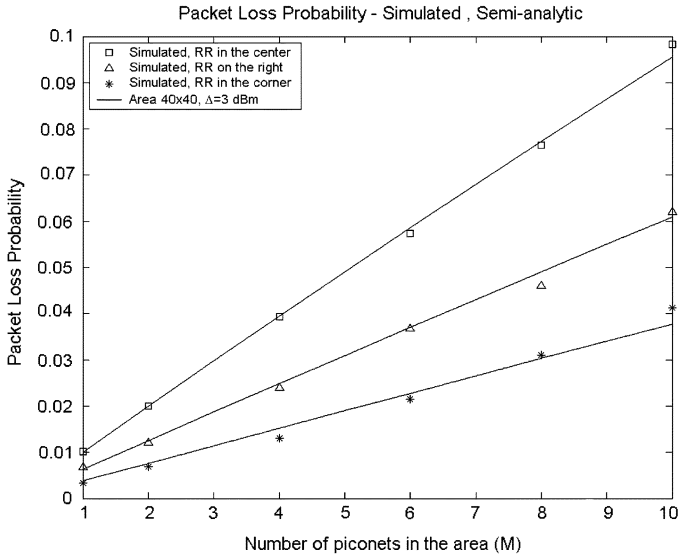

Fig. 5. Packet loss probability versus the number of piconets in the area. Square area: $40 \times 40\ \mathrm{m}^2$, synchronized piconets.

U were set to $W_T = 0\ \mathrm{dBm}$. The histogram bins were assumed to be $\Omega_k = [\Pi_k, \Pi_k + \Delta)$. The grid steps Δx and Δy were assumed to range between 2 cm and 4 cm, depending on the area dimensions.

In Figs. 4 and 5 a very good agreement between the simulated and the semi-analytical results is indicated. As expected, improving the resolution of the discrete approximation of the pdfs of U and W_R, i.e., reducing the step width Δ, the numerical and semi-analytical results become closer. For simplicity, only the case of $\Delta = 2\ \mathrm{dBm}$ for RR in the center was shown in Fig. 4. However, in the considered case, the not so relevant improvement obtained passing from $\Delta = 3\ \mathrm{dBm}$ to $\Delta = 2\ \mathrm{dBm}$ was achieved at the expense of an increased computation time in the calculation of β_k.

To further validate the proposed approach in Fig. 6, we plot the simulated and the outage probability in (11) in the presence

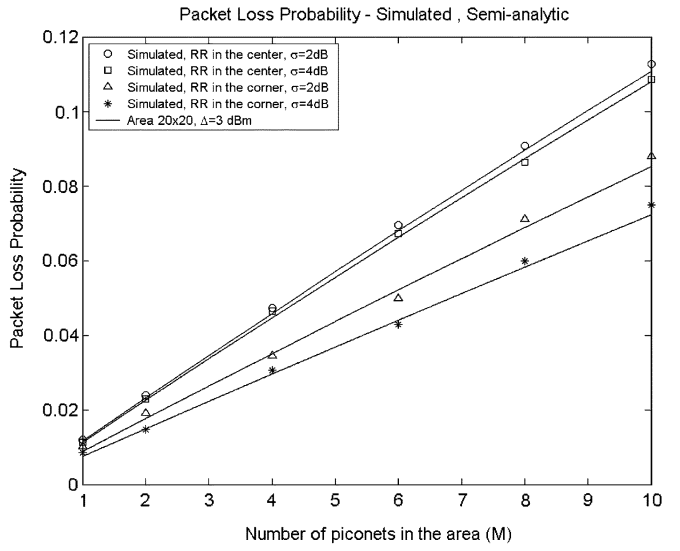

Fig. 6. Packet loss probability versus the number of piconets in the area. Square area: $20 \times 20\ \mathrm{m}^2$, synchronized piconets, $\Delta = 3\ \mathrm{dBm}$, shadowing standard deviations, $\sigma = 2, 4$ dB.

of shadowing. The main effect of shadowing is to reduce the coverage area of the RR depending on the shadowing variance.[5] As indicated in Fig. 6, this leads to a corresponding reduction of the outage probability with respect to the no-shadowing case, when passing from $\sigma = 2\ \mathrm{dB}$ to $\sigma = 4\ \mathrm{dB}$.

B. Packet Loss Probability

In this subsection, we analyze the behavior of the PLP by varying the position of the RR in the network area, and the dimensions of the area where the RR and the interferers are located. We consider the path loss model in (32) and the dimensions of the area are varied from $20 \times 20\ \mathrm{m}^2$ to $40 \times 40\ \mathrm{m}^2$.

In Fig. 7, we plotted the PLP as a function of the number of piconets considering different dimensions of the service area. From Fig. 7, it is observed that when the dimensions of the area are comparable with the Bluetooth terminals coverage area, the PLP is practically independent of the position of the RR (continuous lines in Fig. 7). Increasing the dimensions of the area, effects due to propagation become important and large variations of the PLP with the RR position are evidenced. The plots in Fig. 7 also provide the maximum and the minimum PLP in the area. In fact, it is straightforward to observe that the maximum and the minimum value for the PLP are always obtained when RR is in the center and in the corner, respectively (see Fig. 1). Indeed, the results shown in Fig. 7 for a $20 \times 20m^2$ area are similar to the upper-bound in [8] that was obtained by neglecting every possible mitigation effect due to distance.

In Fig. 8, we plot the outage probability as a function of the number of interfering masters in the area considering three different conditions: synchronized and nonsynchronized piconets. In the latter, we assumed packet duration equal or lower than

[5]In the presence of shadowing, the coverage area of the RR is evaluated starting from the receiver sensitivity and assuming a link margin corresponding to a link reliability of 90%. Thus, for terminals inside the RR coverage area, interference from other piconets is the main source of signal to noise ratio degradation experienced in the RR, and this is accounted for by the outage probability in (11) when the parameters are calculated as in (18).

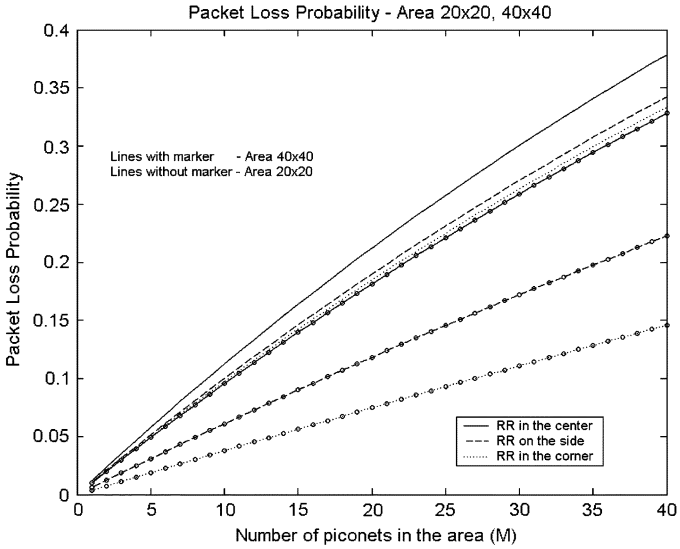

Fig. 7. Packet loss probability versus number of piconets in the area. Square area $20 \times 20\ \mathrm{m}^2$ and $40 \times 40\ \mathrm{m}^2$,synchronized case, different positions of the RR in the area.

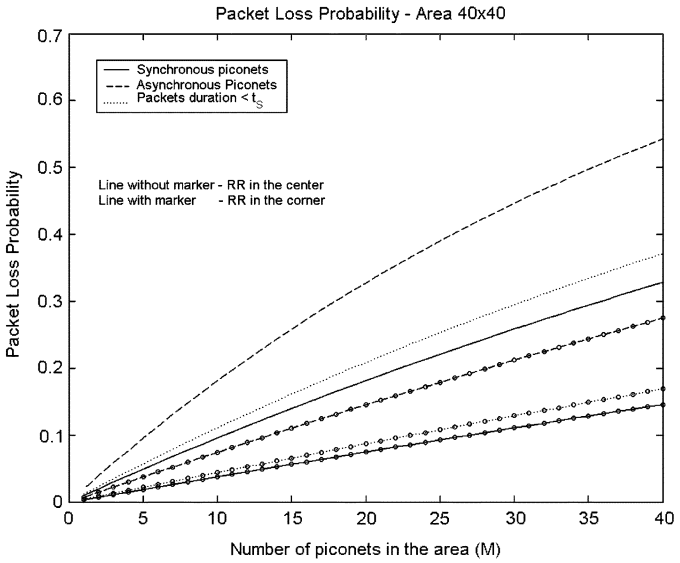

Fig. 8. Packet loss probability versus number of piconets in the area. Square area $40 \times 40\ \mathrm{m}^2$, synchronized, nonsynchronized, and packet length lower than time slot, collision events.

the time slot t_S. In the latter case, the ratio between the packet duration and t_S was $\lambda = 366/650$. As expected, the nonsynchronized case gives the worst PLP results.

The plots in Fig. 7 and Fig. 8 were obtained considering the β_k in Table I. The dependence of β_k on the standard deviation of the shadowing is evidenced by the results in Table II. Data in Table II were used to evaluate (11) to obtain the results in Fig. 6 that validated the proposed approach in the presence of shadowing. The lower values for β_k have been obtained for RR in the corner and for $\sigma = 4$ dB.

Finally, to prove evidence the dependence of β_k and thus of the outage probability on the channel model and, in general, on the propagation characteristics of the selected environment we calculated the β_k assuming

$$L(d) = \begin{cases} 0, & d < 0.1\ \mathrm{m} \\ c_0 + 10\gamma \log_{10}(d), & d \geq 0.1\ \mathrm{m} \end{cases} \qquad (33)$$

TABLE I
VALUES OF β_k USED IN (11), RR IN THE CENTER AND IN THE CORNER OF THE NETWORK AREA,TO EVALUATE THE OUTAGE PROBABILITY IN (11) $\beta_k = 1$ FOR $k > 6$ WERE ASSUMED

β_k/Area	20m x 20m		20m x 10m		40m x 40m	
	Center	Corner	Center	Corner	Center	Corner
β_1	0.9458	0.8082	0.9430	0.8302	0.7920	0.3012
β_2	0.9805	0.9220	0.9796	0.9468	0.9166	0.5579
β_3	0.9859	0.9549	0.9857	0.9751	0.9555	0.7058
β_4	0.9896	0.9574	0.9873	0.9849	0.9691	0.7835
β_5	0.9937	0.9598	0.9885	0.9879	0.9716	0.8614
β_6	0.9958	0.9621	0.9942	0.9912	0.9746	0.9165

TABLE II
VALUES OF β_k, TWO-SLOPE CHANNEL MODEL AND LOG-NORMAL SHADOWING WITH $\sigma = 2, 4$ dB, RR IN THE CENTER AND IN THE CORNER OF THE NETWORK AREA, TO EVALUATE THE OUTAGE PROBABILITY IN (11) $\beta_k = 1$ FOR $k > 6$ WERE ASSUMED

β_k/Area	20m x 20m			
	Center	Center	Corner	Corner
σ	2dB	4dB	2dB	4dB
β_1	0.9233	0.8983	0.6807	0.5693
β_2	0.9801	0.9719	0.8895	0.8209
β_3	0.9838	0.9823	0.9353	0.8893
β_4	0.9917	0.9883	0.9609	0.9297
β_5	0.9923	0.9897	0.9721	0.9425
β_6	0.9965	0.9902	0.9845	0.9631

where $c_0 = -10\gamma \log_{10}(d)$ for $d = 0.1$ m and γ the path loss exponent. No shadowing is considered and results are indicated in Table III. By varying the path loss exponent large variations in β_k and thus, in the outage, probability are observed. By increasing γ from 2 to 4, the reduction in the RR coverage area (from 316 m for $\gamma = 2$ to 5.3 m for $\gamma = 4$) leads to a reduction of outage probability and then of β_k and, as expected, the reduction is more significant for RR in the corner.

C. Network Performance

We still consider a rectangular piconets area, and the propagation model in (32). In this case, the minimum PLP is obtained when the RR is placed in the corner and the maximum PLP is obtained when the RR is placed in the center. We introduce the normalized aggregate throughput defined as $T(M)/C$ where $T(M)$ is given in (23). In Fig. 9, we plot the upper and lower bounds of $T(M)$ in (24) as a function of the number of piconets for different dimensions of the area and considering the nonsynchronized piconets case. From Fig. 9, we observe that increasing the number of piconets, the average normalized Bluetooth network throughput increases as well until a critical value of piconets is reached. Above this value, the overall throughput is reduced due to interference caused by the large number of collisions. In Fig. 9, we can also observe effects of the PLP variability on the network throughput. When the network area is of the same order of the RR coverage area, it is possible to adopt the PLP upper bound in (13) to evaluate the network throughput.

TABLE III
β_k, ONE-SLOPE CHANNEL MODEL, $\gamma = 2, 3, 4$—RR IN THE CENTER AND IN THE CORNER OF THE NETWORK AREA, $40 \times 40\ \mathrm{m}^2$

β_k/**Area**	**40m x 40m**					
	Center	Center	Center	Corner	Corner	Corner
γ	2	3	4	2	3	4
β_1	0.9525	0.8784	0.1050	0.9524	0.5468	0.0262
β_2	0.9825	0.9424	0.2043	0.9824	0.7804	0.0518
β_3	0.9889	0.9608	0.3098	0.9888	0.8554	0.0774
β_4	0.9910	0.9659	0.3946	0.9909	0.8899	0.1013
β_5	0.9942	0.9698	0.4723	0.9940	0.9321	0.1624
β_6	0.9953	0.9721	0.5465	0.9943	0.9754	0.2312

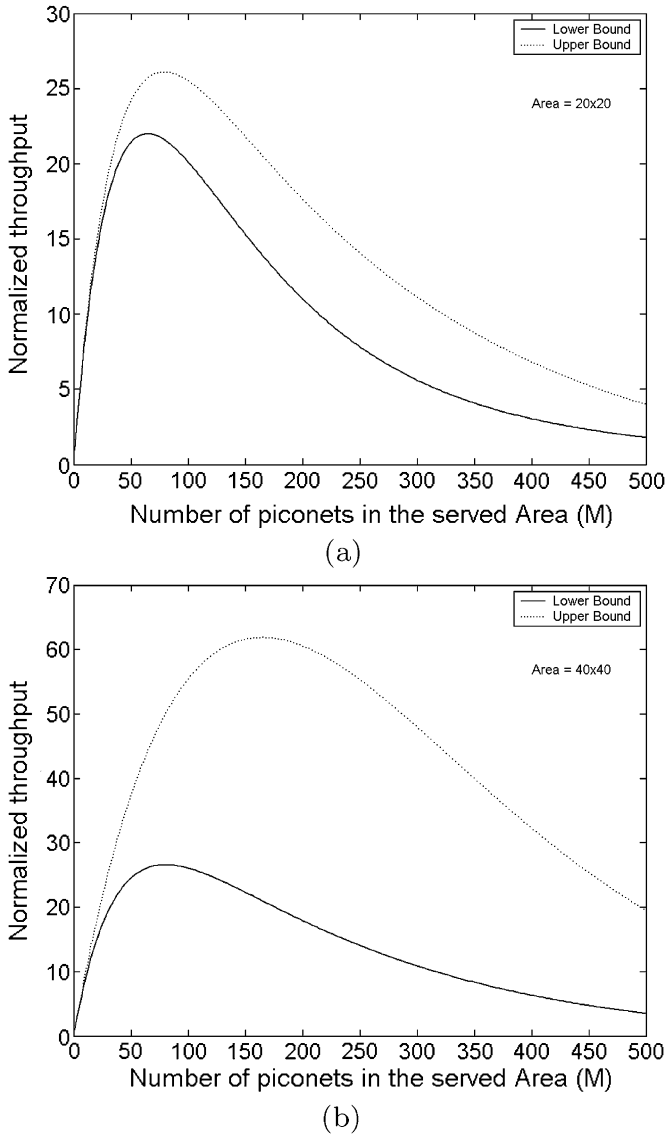

Fig. 9. Normalized Bluetooth network throughput versus the number of piconets, upper and lower bounds, network area dimensions: (a) 20 m × 20 m; (b) 40 m × 40 m.

This is no longer true for larger network areas where the difference between the upper and lower bounds of the throughput can be relevant [see Fig. 9(b)] since the mitigation effects due to the environment cannot be neglected. In this case, the upper bound in [3] and [8] is inaccurate.

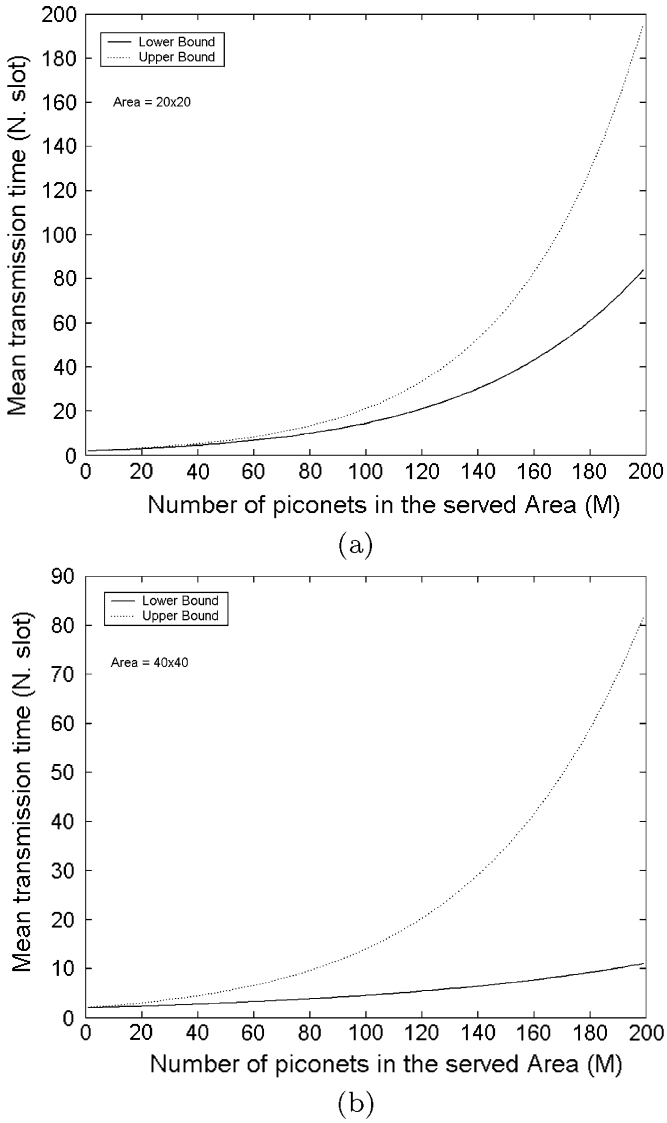

Fig. 10. Upper and lower bounds for the average transmission time vs the number of piconets, area dimensions: (a) 20 m × 20 m; (b) 40 m × 40 m, master-to-slave direction.

In Fig. 10, we plot the upper and the lower bound of the average transmission time expressed as the average number of slots required to deliver a packet. The results in Fig. 10 were obtained considering the master-to-slave direction. The average packet transmission time in the slave-to-master direction can be easily obtained scaling the curves in Fig. 10 by the number of slaves N_S in the piconets, as in (31).

V. CONCLUSION

We presented a novel semi-analytical procedure to evaluate the packet loss probability in Bluetooth networks accounting for the mitigation effects due to the environment geometry and to its propagation characteristics. PLP was subsequently used to evaluate the upper and the lower bounds of some important network parameters such as the network aggregate throughput and the average packet transmission time. The PLP results are

in good agreement with the PLP obtained through Monte Carlo simulations. We showed that the geometry and the propagation characteristics of the environment greatly influences the PLP. In particular, we also discussed on the sensitivity of the PLP with the RR position and it was observed that when the dimensions of the piconets area are comparable with the coverage area of the RR, effects due to propagation are practically negligible. In this case, synchronized and nonsynchronized piconet transmissions with packet duration lower than time slot yield almost the same PLP. Instead, when the area dimensions are larger than the terminal coverage area, the case of synchronized piconets yields better performance, and PLP significantly changes with the RR position. PLP was used to evaluate the upper and the lower bounds of the network aggregate throughput and of the average packet transmission time. Their large variations with the area dimensions as compared to the RR coverage area were evidenced.

Appendix A
Calculation of (11)

In this appendix, we illustrate the derivation of (11). For brevity, we reobtain (11) in the case of $M = 2$ but the extension to generic M is straighforward.

In the case of $M = 2$, the pdf of the rv Z_2 is from (9)

$$f_{Z_2}(x) = f_{W_R}(x) \otimes \left(q\delta(x) + \frac{p}{\rho_0} f_U\left(-\frac{x}{\rho_0}\right)\right) \otimes \left(q\delta(x) + \frac{p}{\rho_0} f_U\left(-\frac{x}{\rho_0}\right)\right). \quad (34)$$

Equation (34) can be rewritten as

$$f_{Z_2}(x) = q^2 f_{W_R}(x) + 2\frac{pq}{\rho_0} f_{W_R}(x) \otimes f_U\left(-\frac{x}{\rho_0}\right) + \frac{p^2}{\rho_0^2} f_{W_R}(x) \otimes f_U\left(-\frac{x}{\rho_0}\right) \otimes f_U\left(-\frac{x}{\rho_0}\right). \quad (35)$$

The outage probability $P(2)$ is achieved by integration of (35) in $(-\infty, 0)$. Observing that $\int_{-\infty}^{0} f_{W_R}(x)dx = 0$, we obtain

$$P(2) = 2qp\beta_1 + p^2\beta_2 \quad (36)$$

where, from (35)

$$\beta_1 = \frac{1}{\rho_0} \int_{-\infty}^{0} f_{W_R}(x) \otimes f_U\left(-\frac{x}{\rho_0}\right) dx$$

$$\beta_2 = \frac{1}{\rho_0^2} \int_{-\infty}^{0} f_{W_R}(x) \otimes f_U\left(-\frac{x}{\rho_0}\right) \otimes f_U\left(-\frac{x}{\rho_0}\right) dx. \quad (37)$$

Appendix B
Numerical Approximation for $f_U(x)$ and $f_C(x)$

We introduce the rv $U = W_T LS$ modeling the interference power due to a transmitter at distance d from the RR, L is the path loss and we assume that the pdf of the shadowing S, $f_S(x)$, is known. Users are randomly located in the area. For calculation purposes we approximate U as a discrete rv assuming a finite set of values $\{\Pi_1, \Pi_2, \ldots, \Pi_K\}$ with probabilities $\pi_1, \ldots, \pi_K$, respectively, i.e.,

$$f_U(x) = \sum_{k=1}^{K} \pi_k \delta(x - \Pi_k). \quad (38)$$

The probabilities π_k depend on the position of the RR and on the physical characteristics of the area described by the path loss model $L = L(d)$. In this Appendix we evaluate π_k using a procedure suitable for computer calculations, assuming a fixed position for the RR. The probabilities π_k are defined as

$$\pi_k = Prob\{U \in \Omega_k\}, \quad k = 1, \ldots, K \quad (39)$$

where Ω_k is the power interval $[\Pi_k - \Delta_k^{(low)}, \Pi_k + \Delta_k^{(up)})$ centered in Π_k and $\Delta_k^{(low)}$, $\Delta_k^{(up)}$ define the lower and the upper limit of Ω_k, respectively. The $\Delta_k^{(low,up)}$ can be selected to have a superset of disjoint sets Ω_k covering the considered power interval. In our derivations, we assumed $\Delta_k^{(low,up)} = \Delta$. Equation (39) can be expressed as

$$\pi_k = \int\int \Xi(x, y | U \in \Omega_k, (x, y) \in S_A)\, g(x, y) dx dy, \quad (40)$$

where $\Xi(x, y | U \in \Omega_k, (x, y) \in S_A)$ is an indicator function identifying the points in the piconets area (S_A) such that the power U, received by the RR, lies in Ω_k. The function $g(x, y)$ is the pdf of the interferer position. The integral in (40) can be calculated using the following numerical approximation. We grid the area as illustrated in Fig. 2 and we fix the position of the RR. For each point in the grid, we evaluate the power U received at the RR using the selected path loss model $L(d)$ and randomly generating the shadowing S according to the pdf $f_S(x)$. Then we arrange the calculated values for U in a histogram whose bins are $\{\Omega_k\}$. The probabilities π_k are obtained from the fraction of samples collected within each bin of the histogram. If we vary the position of the RR in the area, the statistical distribution of distance d changes, leading to a different histogram for U. Therefore, the probabilities π_k depend on the position of the RR and they need to be recalculated when the position of the RR changes. Using a rectangular uniformly-spaced grid with steps Δx, Δy along the x axis and the y axis, respectively, and assuming a uniform distribution of the users in the local service area, i.e., $g(x, y) = 1/A$, where A is the surface area, then the approximation in (16) for (40) holds. The presence of obstacles in the area restricts the possible positions of the interferers and of the RR in the area and this can be accounted for in $g(x, y)$. Similarly, the received power W_R can be expressed as $W_R = W_T LS$, where now d is the distance between the RR and the transmitter in the same piconet. Again, we discretize the power W_R on J levels $\{\Gamma_1, \Gamma_2, \ldots, \Gamma_J\}$, with corresponding probabilities $\gamma_1, \gamma_2, \ldots, \gamma_J$ thus, obtaining (17). To evaluate γ_j, $j = 1, \ldots, J$ we use the same approach as in (16), observing

that the indicator function Ξ in (18) now accounts both for the local piconets area S_A and for the coverage area C_A of the RR.

After some preliminary trials, we observed that to obtain reliable histograms to be used in the derivation of $f_U(x)$ and also $f_C(x)$, a minimum of 1000×1000 points in the grid corresponding to vertical and horizontal distances between adjacent points of 4 cm for the $40 \times 40\ \mathrm{m}^2$ area, in both directions, are required.

ACKNOWLEDGMENT

The authors wish to thank Prof. A. Mecozzi for collaborating in devising (11).

REFERENCES

[1] J. C. Haartsen, "The Bluetooth radio system," *IEEE Personal Comm.*, pp. 28–36, Feb. 2000.
[2] Specification of the Bluetooth System: Core, Version 1.1, Feb. 22, 2001.
[3] Y. Lim, J. Kim, S. L. Min, and J. S. Ma, "Performance evaluation of the Bluetooth-based public internet access point," in *IEEE Proc. 15th Int. Conf. Inf. Networking, 2001.*, Jan. 31–Feb. 2 2001, pp. 643–648.
[4] S. Zürbes, W. Stahl, K. Matheus, and J. Haartsen, "Radio network performance of Bluetooth," in *Proc. IEEE Int. Conf. Commun.*, vol. 3, June 18–22, 2000, pp. 1563–1567.
[5] A. Das, A. Ghose, A. Razdan, H. Saran, and R. Shorey, "Enhancing performance of asynchronous data traffic over the Bluetooth wireless ad-hoc network," in *Proc. 20th Annu. Joint Conf. IEEE Comput. Commun. Soc.*, vol. 1, Apr. 22–26, 2001, pp. 591–600.
[6] A. Karnik and A. Kumar, "Performance analysis of the Bluetooth physical layer," in *IEEE Int. Conf. Pers. Wireless Commun. 2000* , Dec. 17–20, 2000.
[7] D. M. Cordeiro, D. Sadok, and D. P. Agrawal, "Piconet interference modeling, performance evaluation of Bluetooth MAC protocol," in *IEEE Globecom 2001*, vol. 5, Nov. 2001, pp. 2870–2874.
[8] A. El-Hoiydi, "Interference between Bluetooth networks—upper bound on the packet error rate," *IEEE Commun. Lett.*, vol. 5, pp. 245–247, June 2001.
[9] F. Mazzenga, D. Cassioli, P. Loreti, and F. Vatalaro, "Evaluation of packet loss probability in Bluetooth networks," in *IEEE Int. Conf. Commun. (ICC)*, vol. 1, April 28–May 2 2002, pp. 313–317.
[10] A. Papoulis, *Probability, Random Variables and Stochastic Processes*. New York: McGraw Hill, 1965.
[11] J. Haartsen and S. Mattisson, "Bluetooth—A new low-power radio interface providing short-range connectivity," *Proc. IEEE*, vol. 88, pp. 1651–1661, Oct. 2000.

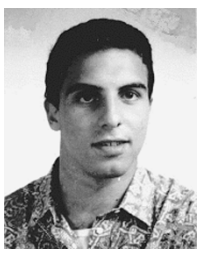

Franco Mazzenga received the Dr. Ing. degree (cum laude) degree in electronics engineering from the University of Rome "Tor Vergata," Rome, Italy. He received the Ph.D. degree in telecommunications from the University of Rome "Tor Vergata," in 1996, discussing a thesis on "Parameter estimation of cyclostationary processes for multi-user spread spectrum systems."

From 1993 to 1994, he was with Fondazione Ugo Bordoni (FUB), involved in radio propagation at millimeter waves. From 1998 to 2000, he was a Researcher at the Consorzio di Ricerca in Telecomunicazioni (CoRiTeL), while still collaborating with the Electronic Engineering Department, the University of Rome "Tor Vergata," where he is presently an Assistant Professor. He is also the Technical Director of Radiolabs, Rome, Italy, doing research on the Bluetooth, UWB, and on software radio topics. His main research interests are in statistical signal processing, multiple access radio techniques, and estimation theory applied to telecommunications.

Dr. Mazzenga was awarded the prize for the 40th year of the FUB, Rome, Italy for his thesis.

Dajana Cassioli (S'02–M'04) received the "Laurea" degree in electronic engineering and the Ph.D. degree in telecommunications and microelectronic engineering from the University of Rome "Tor Vergata," Rome, Italy, in 1999 and 2003, respectively.

From 1998 to 1999, she was with the Fondazione Ugo Bordoni, Rome, Italy, where she was involved in the study of semiconductor optical amplifiers and in the development of computer models of devices for WDM optical communication systems. In 1999, she joined the Communication Group of the Electronic Engineering Department, University of Rome "Tor Vergata," Rome, Italy, where she has been working on the analysis and simulation of the TD-CDMA Radio Interface of the UMTS system. She is currently with the same department, where she is the Project Manager of the UWB technology research activities of RadioLabs, a Consortium between the Electronic Engineering Department of the University of Rome Tor Vergata and three Italian companies operating in the field of wireless communications. She is also the scientific officer responsible in RadioLabs for the IST project ULTRAWAVES, Contract n. IST-2001-35189, funded by the European Community within the Fifth Framework. Her main research interests are in the field of wireless access technologies, and in particular, the UWB radio technology, ad-hoc networks, and Bluetooth. In the year 2000, she was a Summer Manager with the Wireless Systems Research Department at AT&T Labs-Research, working on the statistical analysis of UWB signal propagation.

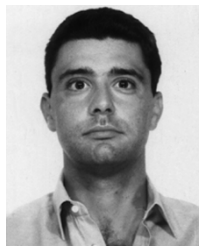

Andrea Detti received the degree in telecommunication engineering from the University of Rome "La Sapienza" Rome, Italy, in 1998 and the Ph.D. degree in microelectronic and telecommunications from the University of Rome "Tor Vergata," Rome, Italy.

In September 2002, he joined the CNIT consortium, as a researcher within the Italian VICOM project. His current research interests focus on transport layer for in ad-hoc environment, peer-to-peer networking, and middleware architecture for context-aware services.

Ibrahim Habib received the B.Sc. degree from Ain Shams University, Cairo, Egypt, in 1981, the M.Sc. degree from Polytechnic University of New York, in 1984, and the Ph.D. degree from the City University of New York in 1991, all in electrical engineering.

From 1981 to 1983, and from 1984 to 1988, he was a Computer Networks Engineer involved in the planning, system engineering, and installation of several IBM SNA networking projects in Egypt and Saudi Arabia. In 1991, he joined the Faculty of the City University of New York, where is now an Associate Professor. From 1998 to 2001, he was also a consultant at the industry; first with AT&T, and then with Telcordia Technologies. His industrial experience spans different areas of data networking such as architecture solutions for IP/WDM networks, IP quality of service architecture, radio resources management in wireless networks, and designing strategies for integrating optical control plane and OSS in IP optical networks. His research interests include traffic engineering in IP and optical networks, wireless LANs, and radio resources management. He has published more than 70 technical papers and reports in those areas.

Dr. Habib was a Guest Editor of the IEEE JOURNAL ON SELECTED AREAS IN COMMUNICATIONS in 1997, and 2000, and a Guest Editor of the IEEE Communications Magazine in 1995 and 1997. From 1994 to 1997, he served as an Editor of the IEEE Communications Magazine. He was Guest Editor of the John Wiley Journal on *Wireless Communications and Mobile Computing* in 2002, and is currently an Editor of the same Journal. He was also a Guest Editor of IEEE Journal on Selected Areas in Communication, Special Issue on Metro Optical Networks, October, 2004. He was the Co-Chairman of the Wireless Networking and Optical Networking Symposia at the IEEE GLOBECOM 2002, and the High Speed Networking Symposium at ICC 2002. He has also served as the Chairman of the Optical Network Symposium, IEEE GLOBECOM 2003 and the Wireless Networking Symposium at ICC 2004. He is listed in the *Marquis Who Is Who in the World* in 2001 and 2004, and *Who's Who in America* 2002, 2003, and 2004 editions.

Pierpaolo Loreti received the Dr. Ing. degree in electronic engineering (cum laude) and the Ph.D. degree in telecommunications and microelectronics from the University of Rome "Tor Vergata", Rome, Italy, in 1998 and 2002, respectively.

Since 1998, he has been collaborating with the Department of Electronic Engineering, the University of Rome Tor Vergata, Rome, Italy. He has worked on several European and National Project such as IST-SUITED and IST-ACCORD. In the 2000, he was with the University of California, Los Angeles, where he worked on Internet application via satellite constellations. In 2002, he worked with the "Consorzio Università Industria-Laboratori di Radiocomunicazioni" (Radiolabs) on technology for the SOHO environment. Since September 2002, he has been a Researcher of "Consorzio Nazionale Interuniversitario per le Telecomunicazioni" (CNIT) working on the Virtual Immersive Communication (VICOM) project powered by Italian ministry of University. His current interests include wireless solutions for SOHO environment, ad-hoc networks, context aware communication, and ambient intelligence.

Francesco Vatalaro (M'85–SM'91) received the Dr. Ing. degree in electronics engineering from the University of Bologna, Italy, in 1977.

He was with Fondazione Ugo Bordoni, FACE Standard, and Selenia Spazio, Italy. In 1987, he became an Associate Professor of radio systems at the University of Roma "Tor Vergata," Rome, Italy, where he is presently a Professor. In 1998, he was a Visiting Professor at the University of Southern California, Los Angeles, and in 2000, was a Visiting Professor at the University of California, Los Angeles. Since 1985, he collaborates in and coordinates several telecommunications projects within national Italian and European programmes. He is the author of about 150 scientific papers. He is a member of the Editorial Board of the *International Journal of Satellite Communications*.

Dr. Vatalaro was a co-winner of the 1990 "Piero Fanti" INTELSAT/Telespazio international prize. He is the Chairman of the IEEE Joint Vehicular Technology/Communications Society Italy Chapter, and is a member of several Scientific Committees in Italy.